THE STUDY OF A CALCULATION METHOD FOR MEASUREMENT OF DIAGNOSTIC NEUTRAL BEAM PROPERTY *

L. Z. liang, C. D. Hu, J. L. Wei, ASIPP, Hefei, China

Abstract

Considering the beam divergence and the convergence of the spherical electrode, the beam transmission model is presented, and the variation of beam edge is described by a formula, which is used to calculate the beam divergence half-angle with the experimental data obtained by the thermocouples. Assuming the beam divergence half-angle is constant in space and time, the beam profile distribution formula and variation of beam axial intensity are introduced. Taking the HT-7 Diagnostic Neutral Beam (DNB) as a reference, the divergence half-angle is calculated for the neutral beam shot 60901. The *1/e* half-width of beam at collimation target calculated by formula is in agreement with that of experimental data. Variation of beam edge and axial intensity with downstream distance is estimated for HT-7 diagnostic neutral beam.

INTRODUCTION

Diagnostic neutral beam is used as active probe. For magnetically confined plasma, neutral particles travel freely across the confining magnetic field. Thus, it is possible to use neutral particles for plasma diagnostic. Combined with Charge eXchange Recombination Spectroscopy (CXRS), plasma rotation velocity, ion temperature, low-Z impurities transmission and so on can be calculated [1,2]. In order to get the optimal signal, the spherical electrode is used for the production of convergent beam.

Accurate knowledge of the beam property, such as beam profile, beam edge and beam intensity, is important for beam transmission and injection into the magnetic confined fusion device. At the same time, the variation of beam edge and axial intensity is a key issue for the design and operation of diagnostic neutral beam. The size of beam spot is a guide for design of the internal components and depositing power at the inner elements.

In this paper, the formula of beam edge is given with divergence angle and the convergence angle. The beam profile distribution is taken as a Gaussian distribution, and the formula is employed with the divergence half-angle and downstream distance. The formulas have been applied to HT-7 DNB. Variation of beam edge and axial intensity, the beam profile at calorimeter location are reported.

CALCULATION METHOD ANALYSIS

The production of neutral beam and the basic elements are shown in Fig.1. The source plasma is generated by filaments cathode and anode bucket with the confinement of permanent magnet. As the required beam energy increases, the multi-stage geometry is used to boost the ions of source plasma with electrostatic field, as show in Fig.1. The first gap in the extraction system is for pre–acceleration. The second gap post-accelerates the ion beam to a desired level. The third gap is to suppress the electrons of the gas-cell neutralizer plasma from back-accelerated beams. Thus, the trajectory of ion is restricted by the electrostatic field and aperture in every extraction grid. The beam-let will be formed after the exit grid, and it will be a convergent beam-let or a parallel beam-let or a divergent beam-let due to the different perveance employed on the grid. After the exit grid, the neutralizer gas allows the neutralization of beam ions by charge exchange. The neutralization efficiency is up to 80% for deuterium at 50 keV [3,4]. Consequently, in the space without the electromagnetic field, ignoring the space charge effect, the trajectory of energetic neutrals motion will be a line.

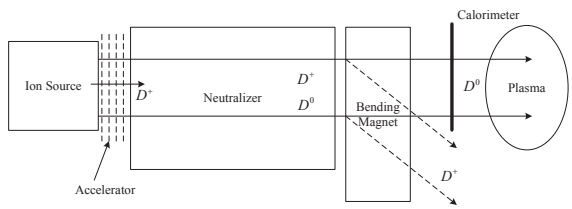

Figure 1: Layout of diagnostic neutral beam injector.

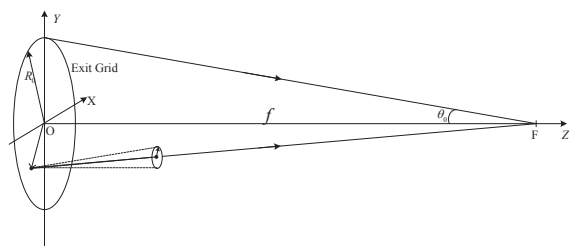

Figure 2: Coordinate system for convergent neutral beam.

The extraction area in spherical electrode is considered as a reference, and the focal distance is *f*. The coordinates for this extraction system is shown in Fig.2. The emitting surface is set in XOY plane, the beam axis is set as Z axis and three axes are in right hand law. The radius of emitting surface is marked as R_0 with a convergence angle θ_0. For this axis-symmetrical convergent beam, the model of beam transmission could be taken as shown in Fig.3. The solid line is the axis of beam-let, and the dotted line is edge of beam-let, the outboard lines are the edge of beam. Generally, beam-let, after the extraction grid, is

*Work supported by National Natural Science Foundation of China under Grant No. 11075183.

Copyright © 2013 by JACoW — cc Creative Commons Attribution 3.0 (CC-BY-3.0)

emanative with the divergence half-angle α. Thus, the ideal beam radius of beam will be described as:

$$R(\alpha,z)=\begin{cases}R_0+(-\tan(\theta_0-\alpha))\times z & (z\le f)\\ -R_0+\tan(\theta_0+\alpha)\times z & (z>f)\end{cases} \quad (1)$$

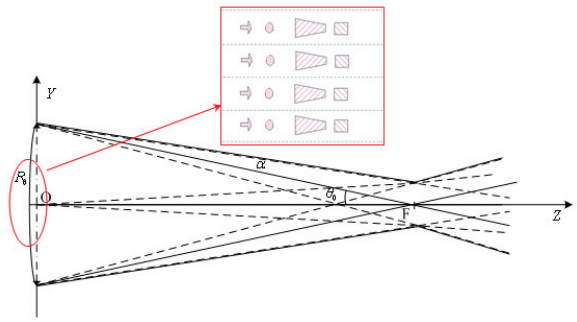

Figure 3: The model of beam transmission.

For arc discharge ion source, it is the uniformity distributed source plasma that we expect for ion beam extraction. Consequently, we assume that the beam intensity distribution at the extraction grid has a uniformity distribution in two-dimensional. Assuming that the beam-let divergence angle is the same, is constant in space and time, and a beam-let pulled from an aperture has a Gaussian distribution in two-dimensional for a certain cross-section. So, we can write the relative intensity distribution of the beam as [5,6]:

$$i(\alpha,r,z)=\frac{1}{\pi a^2}\exp(-\frac{r^2}{a^2}) \quad (2)$$

Where, a is the Gaussian half-width with *1/e* half-angle α. In order to calculate the beam absolute intensity, the normalized coefficient I' is employed,

$$I'=\frac{I}{\int_0^{2\pi}\int_{-a}^{a}\frac{1}{\pi a^2}\exp(-\frac{r^2}{a^2})drd\varphi} \quad (3)$$

Where, I is the total beam power at the calorimeter location, is calculated by the Gaussian fitting.

If there is a calorimeter with the thermocouples downstream, the beam profile could be described with the temperature rise obtained by thermocouples. The beam radius R and the beam power could be evaluated. Using formula (1), the beam divergence half-angle α could be estimated. At the calorimeter location, the normalized coefficient I' is calculated, using formula (2) and (3). For a certain divergence half-angle α, the *1/e* Gaussian half-width α is certain value for certain z. Assuming the beam divergence half-angle α is constant in space and time, using the beam divergence half-angle α and the normalized coefficient I', the beam profile can be estimated, for any location in the downstream, the beam radius can be evaluated by formula (1). Certainly, with this beam profile, beam edge and beam power can be evaluated approximately.

CALCULATION RESULTS FOR HT-7 DNB

HT-7 DNB device includes a bucket ion source with 160*mm* diameter extraction area and long-curvature sphere electrode grids. As a result, the beam-lets from every aperture in extraction grid steer to a common focus, and the focal distance is 2568*mm*. The calorimeter with 13 thermocouples is located at 1362.34*mm* downstream from ion source. At the same time, the collimation target with 10 thermocouples is located at 1741.83*mm* downstream. In normal operation, the DNB can produce 5.5*A* of extracted beam current in hydrogen at an energy of 50keV [7].

The calorimeter with thirteen 2mm diameter holes crossly distributed is cupreous. The distance between each two neighboring holes on a same range is 13.5*mm*. Behind the hole, thirteen thermocouples are embedded in sample copper respectively for temperature rise $\triangle t$ measurement. The beam profile can be described by temperature rise. The beam intensity at the thermocouple location can be calculated by:

$$p=\frac{m\times c\times\int\Delta tdt}{A\times\tau}\ (\mathrm{w/mm^2}) \quad (4)$$

Where, A is the area of the heat flux holes, τ is the duration time of neutral beam, τ=*0.1s*, m is the mass of sample copper, m=*0.52g*, c is the specific heat of copper. The structure of collimation target is similar with that of calorimeter. However, the mass of sample copper is 0.49*g*, the diameter of the heat flux holes is 2.54*mm* [8].

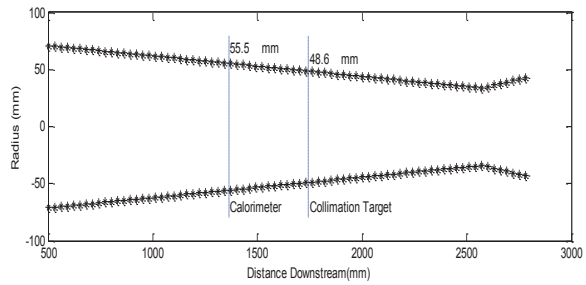

Figure 4: Downstream variation of beam edge.

For shot 60901 and 60903, they are experimented at 44kV/4.4A, working with calorimeter and collimation target respectively. Using the data from the shot 60901, through the Gaussian fitting of the beam intensity profile, the *1/e* half-width of beam is about 55.5 mm at the location of calorimeter. The divergence half-angle can be estimated by formula (1). The calculated divergence half-angle is α=*0.75°*. Thus, variation of the beam edge calculated with formula (1) is shown in Fig.4. The smallest beam spot appeared at the location of the focus position. At the location of collimation target, the calculated beam radius is 48.6mm. By Gaussian fitting the experiment data from collimation target, the beam radius is 47.1mm, which is in agreement with that calculated by formula (1).

Copyright © 2013 by JACoW — cc Creative Commons Attribution 3.0 (CC-BY-3.0)

ISBN 978-3-95450-122-9

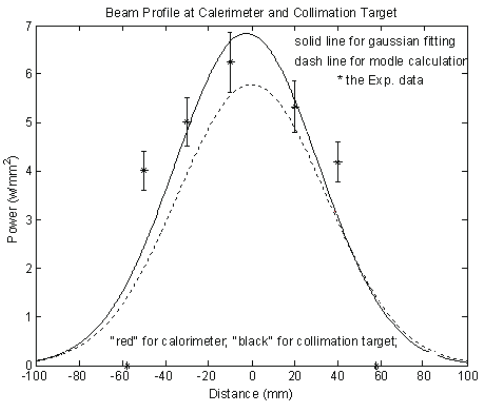

Figure 5: Downstream variation of beam edge.

Using the above method of calculation, we prepared the calculated program. Firstly, the beam power at the calorimeter is valuated using the experiment data. Then, the normalized coefficient I' is estimated, thus the beam profile formula could be written as:

$$i(r,z)=\frac{I'}{\pi a^2}\exp(-\frac{r^2}{a^2}) \qquad (5)$$

Thus, we can estimate the beam profile, as shown in Fig.5. The starts represent power density obtained by experiment, the solid line is the Gaussian fitting result and the dashed line represents calculated results by formula (5) for collimation target with divergence angle evaluated by Gaussian fitting at the location of the calorimeter. Considering the error of thermocouple measurement, the calculated beam profile could be taken as the same with that of Gaussian fitting. Fig.6 shown the variation of beam profile, the dash line represent the beam profile for any location downstream, which are calculated by formula (5)

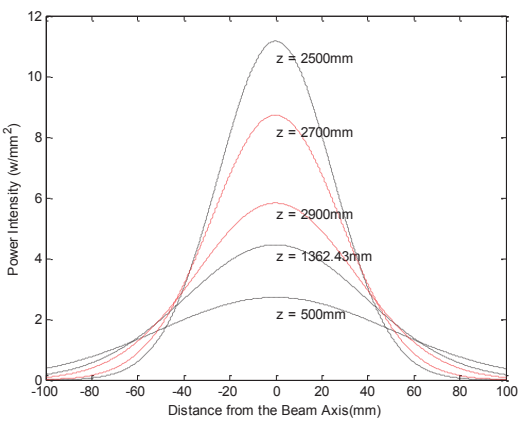

Figure 6: The downstream variation of beam profile.

Using the beam profile, the axial beam intensity and the beam edge intensity are shown in Fig.7. The maximal beam intensity is about $12w/mm^2$ at about 2568mm downstream from ion source. Consequently, if the diagnostic neutral beam interaction with plasma at this location, we can get the optimal signal for CXRS. After this location, the *1/e* width of beam will increase, as shown in Fig.4. Consequently, the beam intensity on z-axis will be getting smaller and smaller, after the maximal beam intensity location.

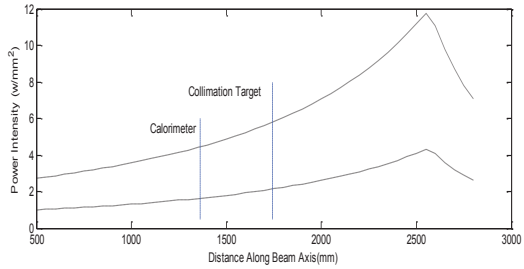

Figure 7: The downstream variation of axial beam intensity.

CONCLUSION AND DISCUSSION

For convergent neutral beam, the calculation method for beam profile is introduced, and the formula of variation of beam edge is presented. It is useful for inner elements design, the injector design and so on. But, one thing should be noted. The assumption about identical divergence half-angle is not appropriate for real system. During operation, the beam divergence angle is affected by the voltage of the electrode, space charge effect and the non-uniformity of source plasma. Besides, it is difficult to confirm space charge effect and the non-uniformity of source plasma as they are time-varying.

The calculation is just a mathematical model. The process of the neutralization and beam transmission can not be displayed in detail, the effect of the bending magnet can not be considered. The divergence angle, beam power and focal distance of the convergent beam are the key parameters for calculation. However, a precise measurement of beam power can not be obtained by calorimeter. The interaction between beam and calorimeter is a complicated process and the time response of the calorimeter is very slow. In this article, we take the beam power evaluated by calorimeter as that emitted from the extraction surface. Thus, using the beam power as a parameter for our program, which is obtained from the calorimeter, the beam intensity measured value will be smaller than the actual beam intensity.

REFERENCES

[1] I. H. Hutchinson. Principles of Plasma Diagnostics. Cambridge: Cambridge University Press, 2002.
[2] L. Q. Hu, et al. Rev. Sci. Instrum, 75(2004): 3496.
[3] E. Speth, Rep. Prog. Phys, 52(1989):57.
[4] F. Melchert, et al., Atoms Molecules and Clusters, 21(1991):S249.
[5] J. Kim, et al., Nuclear instruments and methods, 141(1977):187.
[6] C. Fuentes, et al., Fusion Engineering and Design, 82(2007):5.
[7] Z. M. Liu, et al. Fusion Engineering and Design, 82(2007): 325.
[8] L. Z. Liang, et al. Nuclear Techniques, 32(2009):78.

Copyright © 2013 by JACoW — cc Creative Commons Attribution 3.0 (CC-BY-3.0)